

A Retro-orbital Sinus Injection Mouse Model to Study Early Events and Reorganization of the Astrocytic Network during Pneumococcal Meningitis

Chakir Bello^{1, 2, 3, 4}, Martine Cohen-Salmon^{2, 3, 4, 5} and Guy Tran Van Nhieu^{1, 2, 3, 4, §, *}

¹Team Intercellular Communication and Microbial Infections, Center for Interdisciplinary, Research in Biology, Collège de France, 75005 Paris, France

²Institut National de la Santé et de la Recherche Médicale U1050, 75005 Paris, France

³Centre National de la Recherche Scientifique UMR7241, 75005 Paris, France

⁴MEMOLIFE Laboratory of excellence and Paris Science Lettre

⁵Team Physiology and physiopathology of the Gliovascular Unit, Center for Interdisciplinary, Research in Biology, Collège de France, 75005 Paris, France

§Present address: Inserm U1282- CNRS UMR8113, Ecole Normale Supérieure Paris-Saclay, Gif-sur-Yvette, France

*For correspondence: guy.tran_van_nhieu@ens-paris-saclay.fr

[Abstract] Pneumococcal (PN) meningitis is a life-threatening disease with high mortality rates that leads to permanent neurological sequelae. Studies of the process of bacterial crossing of the blood brain barrier (BBB) are hampered by the lack of relevant *in vitro* and *in vivo* models of meningitis that recapitulate the human disease. PN meningitis involves bacterial access to the bloodstream preceding translocation across the BBB. A large number of PN meningitis models have been developed in mice, with intravenous administration via the lateral tail vein representing the main way to study BBB crossing by PN. While in humans, meningitis is not always associated with bacteremia, PN meningitis after intravenous injection in mice usually develops following sustained and very high bacteremic titers. High grade bacteremia, however, is known to favor inflammation and BBB permeabilization, thereby increasing PN translocation across the BBB and associated damages. Therefore, specific processes associated with early events of PN translocation may be blurred by overall changes in the inflammatory environment and potentially systemic dysfunction in the case of severe sepsis. Here, we report a mouse meningitis model induced by PN injection in the retro-orbital (RO) sinus. We show that, in this model, mice appear to control bacteremic levels during the first 13 h post-infection, while PN crossing of the BBB can be clearly detected by fluorescence confocal microscopy analysis of brain slices as early as 6 h post-infection. Because of the low frequency of events, however, PN translocation across brain parenchymal vessels at early time points requires a rigorous and systematic examination of the brain volume.

Keywords: Pneumococcus, Meningitis, Blood brain barrier, Intravenous, Retro-orbital sinus

[Background] Bacterial meningitis is a severe disease with high mortality rates and life-long neuropsychological sequelae for survivors. Its incidence is particularly high in low/moderate resources countries (GBD 2016 Meningitis Collaborators, 2018). Only a limited number of bacterial species cause

meningitis, with *Haemophilus influenzae* type b, *Neisseria meningitidis* (meningococcus), and *Streptococcus pneumoniae* (pneumococcus) accounting for the large majority of cases.

Pneumococcus (PN) is a human nasopharyngeal commensal and major bacterial pathogen responsible for invasive diseases (IDs). Its high genomic plasticity accounts for the large number of identified serotypes (>96), with only a minority (<13) associated with invasive diseases such as bacteremia, cellulitis, pneumonia, or meningitis. PN is the main causative agent of community-acquired meningitis, which has high morbidity and mortality worldwide (Mook-Kanamori *et al.*, 2011). Despite the characterization of the role of several PN virulence determinants, the mechanism underlying PN crossing of the BBB remains poorly understood. In particular, among the large number of serotypes, it remains unclear why a limited subset is more frequently associated with meningitis (Kulohoma *et al.*, 2015). PN meningitis is believed to follow bacterial translocation across the nasopharyngeal epithelium and access to the blood stream for sustained periods of time (Iovino *et al.*, 2013).

Despite the recent development of *in vitro* BBB models, a major hurdle remains with the lack of *in vitro* systems that faithfully recapitulate the BBB properties (Abbott *et al.*, 2010; Abbott and Friedman, 2012; Sonar and Lal *et al.*, 2018). This is largely due to the barrier itself, implicating endothelium interplay with astrocytes, mural cells (pericytes and vascular smooth muscle cells), and neurons. Indeed, the barrier “mechanical” properties are conferred by endothelial cells from the brain vasculature forming tightly sealed intercellular junctions, with low and regulated endocytic activity. However, endothelial permeability is controlled by the interaction of astrocytes, via processes called endfeet contacting the perivascular space surrounding intra-parenchymal brain vessels, through the secretion of cytokines and other chemical factors, such as TGF- β , or IL-6 (Abbott and Friedman, 2012). Neurons and pericytes also control endothelial trans-cellular permeability by regulating BBB gene transcription and by promoting astrocyte endfeet polarization around blood vessels (Armulik *et al.*, 2010). In addition, through mechano-sensitive signaling, shear stress induced by blood flow promotes the up-regulation of endothelial intercellular components and transporters required for BBB function (Cucullo *et al.*, 2011). Finally, the cytokinic and inflammatory environment regulated by immune cells locally recruited at infectious sites plays a critical role in BBB permeability (Sonar and Lal *et al.*, 2018). Specifically, microglial cells, acting as a first line of defense, play a key role in controlling infection but may also contribute to BBB permeabilization during systemic inflammation (Gres *et al.*, 2019; Haruwaka *et al.*, 2019). In light of all these considerations, the gold standard to study BBB crossing by pathogens currently remain *in vivo* models with a stable genetic background, such as inbred mice.

Balb/c and C57/BL6, the main mouse models used in infection studies, show different sensitivity to PN infections and PN clones (Sandgren *et al.*, 2005; Jeong *et al.*, 2011). Presumably, because of their weaker Th1-response, Balb/C mice are more sensitive than C57/BL6 mice to systemic PN infections and have been used in various PN meningitis models (Sandgren *et al.*, 2005; Grandgirard *et al.*, 2007; Jeong *et al.*, 2011). Among the various mouse models of PN meningitis, intracranial injection of bacteria in the subarachnoidal space cannot be considered to study PN translocation across the BBB. Other models involve means to fragilize the BBB (e.g., hyaluronidase injection and promoting inflammation) that may alter invasion routes, or cochlear implants leading to PN spreading to the middle, inner ear,

and then CSF. PN meningitis models triggered following intraperitoneal or intranasal injection have also been used. Intravenous injection via lateral tail veins remains a method of choice to trigger PN meningitis, but requires skills and practice. To overcome the drastic bacterial clearance mediated by neutrophils and splenic macrophages during the first hours of infection, a sufficient inoculum needs to be administered intravenously while not exceeding the dose that will trigger septic shock, usually between 10^7 - 10^8 equivalent CFUs (Gerlini *et al.*, 2014). In all aforementioned methods, meningitis occurs following sustained high bacteremic titers ($> 10^6$ CFUs/ml) not always observed in human diseases (Shahum *et al.*, 2007), questioning the links between meningitis and major dysfunctions associated with sepsis in these models.

Intravenous administration by injection in the mouse retro-orbital (RO) sinus was first introduced about 15 years ago as a convenient alternative for tail vein injection and is now routinely used (Yardeni *et al.*, 2011). While it was also used for the intravenous administration of pathogens or toxins, its use to induce bacterial meningitis had not been described previously to our recent works (Bello *et al.*, 2020). Potential leakage from the RO sinus or local inflammation linked to the injection procedure is unlikely because RO injection has been routinely used in studies assessing BBB permeability to various compounds (Zuluaga-Ramirez *et al.*, 2015). Here, we described administration via the RO sinus as a robust and reproducible model to study early events during PN meningitis. Following RO injection, mice reproducibly developed PN meningitis associated with endothelial and systemic inflammation, while showing controlled bacteremic titers (Bello *et al.*, 2020). Interestingly, the bacteremia dynamics appeared to differ from those described for tail vein injection. RO injection of 10^7 CFU-equivalent leads to sustained bacteremic titers (ca. 10^4 - 10^5 CFUs/ml) during the first 13 h post-infection. An abrupt increase to up to 10^8 CFUs/ml after 24 h post-infection may be observed, which likely corresponds to secondary infection from infected organs and systemic failure (Bello *et al.*, 2020). These results suggest that, as opposed to tail vein injection, bacteria injected in the RO sinus are not rapidly diluted in the bloodstream, but steadily released from the retro-orbital sinus during the first hours of infection.

Specifically, this model enables the visualization of early events of PN translocation across brain parenchymal vessels and its effects on astrocytes. While in humans, PN rarely causes encephalitis or meningoencephalitis, our studies indicate that PN translocation in the CSF occurs early and concomitantly with translocation across brain parenchymal vessels, indicating that this model could also be used to study the severe forms of PN meningoencephalitis associated with major brain injury. However, due to the low frequency of PN translocation in the brain at early time points (<6 h post-infection), its visualization by immunofluorescence microscopy requires the systematic analysis of brain slices, which we describe in this article.

Materials and Reagents

1. 1.5 ml Eppendorf tubes safe-lock (Eppendorf, catalog number: 0030120086)
2. 15 ml Falcon tubes (Dutscher, catalog number: 352095)
3. Mouse cages (Animalab, catalog number: 031200260)

4. 0.3 ml Terumo Insulin syringes (Terumo, catalog number: 3BS30M2913)
5. Syringe needles Gauge 27, L ½ inch (Sigma-Aldrich, catalog number: Z192384)
6. Scalpels (Fisher Scientific, catalog number: 3120032)
7. Defibrinated sheep blood (Alliance-bio-expertise, catalog number: 23689)
8. Bacteriological agar (Sigma-Aldrich, catalog number: A5306)
9. Todd Hewitt medium (ThermoFisher, catalog number: BD249240)
10. Yeast extract (ThermoFisher, catalog number: 210929)
11. Phosphate Buffer Saline (PBS)
12. OCT cryoembedding matrix (Fisher Scientific, catalog number: 23-730-625)
13. Isopentane (Sigma-Aldrich, catalog number: PHR1661)
14. Paraformaldehyde (Merck, catalog number: 158127)
15. Ethanol (Merck, catalog number: 493511)
16. Goat serum (Sigma-Aldrich, catalog number: G9023)
17. Triton X-100 (Merck, catalog number: X100)
18. Ketamine (Merck, catalog number: Y0000450)
19. Xylazine (Merck, catalog number: 46995)
20. DAKO (DAKO, catalog number: 83023)
21. Trizol (Invitrogen, Life Technologies, catalog number: 15596026)

Strains:

1. Wild-type serotype 4 *Streptococcus pneumoniae* TIGR4 (ATCC, catalog number: BAA-334™)
2. C57/BL6 6-8-week-old male mice (Charles River)

Antibodies:

1. Anti-PN capsular rabbit polyclonal antibody (Statens Serum Institute, Copenhagen, Denmark).
2. Anti-GFAP mouse monoclonal antibody (ThermoFisher, catalog number: G3893)
3. AlexaFluor 563-conjugated isolectin IB4 (ThermoFisher, catalog number: A11029)
4. AlexaFluor 488-conjugated goat anti-mouse IgG (Life Technologies, catalog number: A11029)
5. AlexaFluor 555-conjugated goat anti-rabbit IgG (Life Technologies, catalog number: A11034/A21429)
6. 6-Diamidino-2-phenylindole dihydrochloride (DAPI) (ThermoFisher, catalog number: D9542)
7. RNeasy Lipid Tissue kit (Qiagen, catalog number: 74804)
8. Superscript II reverse transcriptase kit (ThermoFisher, catalog number: 18064014)
9. SYBR green PCR master kit (ThermoFisher, catalog number: A46012)

Equipment

1. Biosafety level 2 laboratory
2. CO₂ incubator (Sanyo, model: MCO-18AIC)

3. Spectrophotometer (WPA, Biowave)
4. Eppendorf centrifuge (Eppendorf, model: 5810)
5. Eppendorf centrifuge (Eppendorf, model: 5424)
6. Sterile hood (Telstar, Bio II A)
7. Peristaltic pump (Gilson, Minipuls Evolution)
8. 4°C refrigerator (Liebherr, Comfort)
9. Nanodrop (Thermo Scientific, model: NanoDrop 2000)
10. PCR Light Cycler (Roche Life Science, model: LightCycler® 480)
11. Cryostat (Cryostar, model: NX70)
12. TissueLyser II (Qiagen, model: 85300)
13. -80°C freezer (Sanyo, model: MDF-U53V)
14. Inverted fluorescence microscope with motorized XYZ stage (Nikon, model: Eclipse Ti) equipped with a Plan Apo Lambda 60× objective /1.40 NA oil
15. Spinning disk confocal microscope (Roper Scientific) equipped with a Yokogawa CSU-W1 scanner unit, 405 nm, 100 mW – 491 nm, 150 mW – 561 nm, 50 mW – 642 nm, 25 mW lasers, and a C-MOS Camera (Andor, an ORCA-Flash 4.0)

Software

1. Fiji
2. Microsoft Excel
3. Metamorph 7.7

Procedure

A. Pneumococcal culture

1. Streak PN serotype 4 wild-type strain TIGR-4 from a glycerol stock onto a THY 5% blood agar plate. Incubate for 16-24 h in a 10% CO₂ incubator at 37°C.
2. Inoculate 2 ml of THYE pre-culture in a 15 ml sterile Falcon tube with one single colony. Incubate for 16H in a 10% CO₂ incubator without agitation.
3. Inoculate 5 ml of THYE culture with a 1:100 dilution of pre-culture. Incubate in a 10% CO₂ incubator until $0.2 < OD_{600nm} < 0.4$. Because of its capacity to undergo quorum sensing-dependent autolysis, growing PN cultures can be tricky. In particular, the lag phase preceding growth may be of variable duration, sometimes extending over several hours. However, once bacterial growth exceeds $OD_{600nm} > 0.15$, the doubling time may be as short as 15 min. The incubation time for this step will vary but in general should not last more than 4 h.
4. Centrifuge the culture at 21°C for 5 min at 7,000 × g, and discard the supernatant.
5. Resuspend the pellet in 5 ml of sterile PBS.
6. Determine the bacterial density by reading the OD_{600nm}. Because of its capacity to undergo

quorum sensing-dependent autolysis, growing PN cultures can be tricky. In particular, the lag phase preceding growth may be of variable duration, sometimes extending over several hours. However, once bacterial growth exceeds $OD_{600nm} > 0.15$, the doubling time may be as short as 15 min.

7. Centrifuge the culture at 21°C for 5 min at $7,000 \times g$, and discard the supernatant.
8. Adjust the PBS volume to obtain final $OD = 1.0$ (ca. 2×10^8 CFUs/ml). Note that the OD–CFU correspondence may vary depending on the PN strain and may need to be determined empirically.

B. Mice RO injection and sampling (Figure 1)

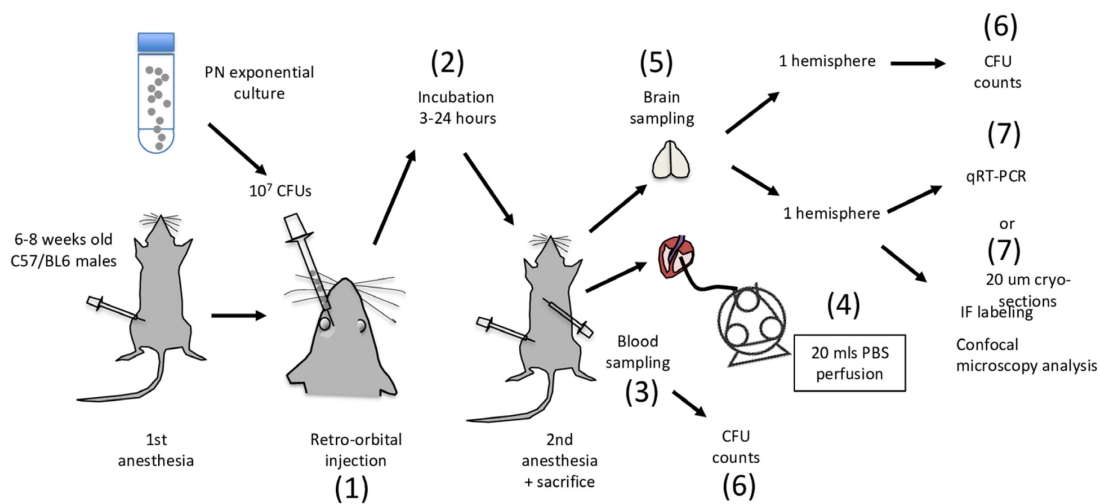


Figure 1. Flow chart of PN meningitis analysis following RO injection in mice.

Major steps are indicated by numbers and are performed in sequential order. Besides step 7, all other steps are performed in a P2 environment. Steps 3-6 are performed in a laminar flow sterile hood.

If mice are not bred on site but delivered from an external supplier, allow mice to adjust in local animal facilities for 3 days prior to experimentation. The day of the experimentation, isolate the mouse subjected to manipulation in the P2 environment from other mice. These measures are to limit potential variations linked to animal stress.

1. Anaesthetise C57/BL6 mice with a intraperitoneal injection of 100 μ l of 10% (vol:vol) ketamine (100 mg/ml) and 2% xylazine in PBS. Use tuberculin syringes with a 27-gauge needle for injections.
2. Inject mice with 50 μ l (10^7 CFUs) of the PN suspension in the RO. The procedure for RO injection is described in detail in reference (Yardeni *et al.*, 2011), with many tutorial videos available online (e.g., <https://www.research.psu.edu/animalresourceprogram/training/videos/retro-orbital-injection-in->

[the-mouse](#)). Briefly, the mouse right eyeball is mildly exorbited by applying gentle pressure on the skin dorsal and ventral to the eye. A drop of ophthalmic anesthetic such as 0.5% proparacaine hydrochloride may be added to prevent eye desiccation. To limit potential damage to the eyeball, the needle is inserted bevel down. Injection and removal of the needle are performed slowly to favor diffusion of the bacterial suspension in the RO sinus.

3. Mice are returned to their cage for the incubation period. Upon awakening, mice are usually active and show few symptoms during the first hours post-infection. Piloerection and slowed activity are clearly detected 9 h post-infection, with prostration and labored breathing after 24 h, time at which mice are sacrificed, then wiped with 70% ethanol.
4. Pin the mouse paws with needles to a board.
5. Cut the skin over the diaphragm.
6. Cut the diaphragm to reveal the thoracic cage. While holding the xiphoid process, cut the ribs on both sides of the thoracic cage.
7. Perform cardiac sampling of blood first for CFU determination [Figure 1 (6)].
8. Perform intracardiac perfusion with 20 ml of sterile PBS to wash away contaminated blood in the organs' vessels. This procedure is described in detail in Wu *et al.* (2021).
9. To this aim, cut the right atrium to allow the flow through of perfused PBS.
10. Insert the 22G-blunt perfusion needle filled with PBS into the left ventricle, towards the aorta.
11. Flow PBS in the tubing using the peristaltic pump until a drop is visible at the tip of the Luer lock connector, to avoid bubbles.
12. Connect the perfusion needle to the Luer lock connector.
13. Flow PBS at 2.5 ml/min for 8-10 min. The mice should become exsanguinated.
14. Open the skull with a scalpel and remove the brain.
15. Pre-weigh empty sterile Eppendorf tubes. Separate the brain hemispheres, transfer each hemisphere to an Eppendorf tube, and weigh immediately. Calculate the weights of the hemispheres.
16. Use immediately for CFU determination. Alternatively, flash-freeze for qRT-PCR or process for confocal microscopy analysis of immunofluorescent labeling of brain slices, as described below.

C. CFU counting (Figure 2)

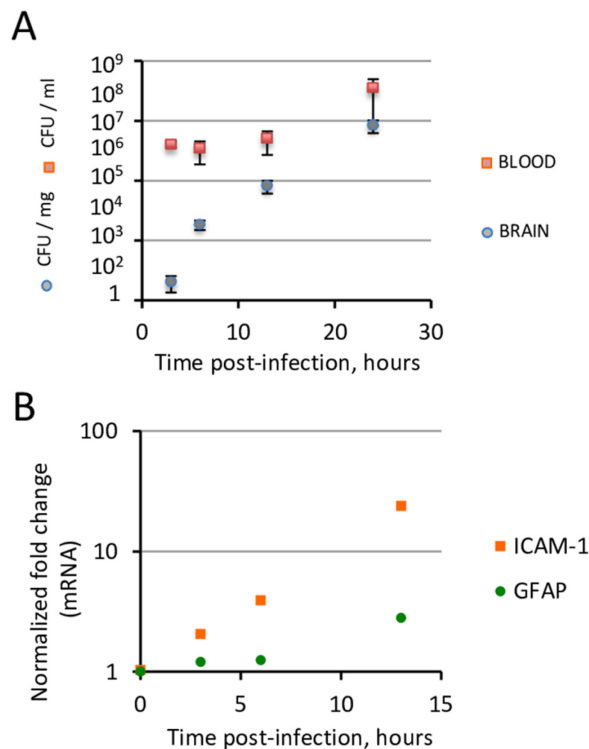


Figure 2. PN translocation across the blood brain barrier occurs under controlled bacteremia during the first hours of infection.

C57/BL6 6-8-week-old mice were injected intravenously with 10^7 PN equivalent CFUs via the RO sinus. At various time points post-infection, mice were sacrificed. **A.** CFU determination from brain and blood samples. Note that during the first 13 h post-infection, bacteremia remains constant (ca. 10^5 CFUs/ml) while brain CFUs increase exponentially. **B.** qRT-PCR analysis of total RNAs from brain samples ($N > 3$ mice per determination). Endothelial and astroglial inflammation assessed by mRNA transcripts of ICAM-1 and GFAP, respectively, show a significant increase at 13 h post-infection.

1. Homogenize the brain hemisphere in 2 ml of sterile PBS.
2. Perform serial 10-fold dilutions of the brain homogenate in PBS. Conveniently, dilutions are performed by serially transferring 10 μ l of homogenate in sterile Eppendorf tubes containing 90 μ l of PBS.
3. Plate 50 μ l of each dilution on a THYE blood agar plate.
4. Incubate for 16-48 h in a 10% CO_2 incubator at 37°C.
5. Count CFUs and normalize to the dilution factor and brain weight.

D. qRT-PCR (Figure 2)

Hemispheres are either processed immediately or flash-frozen in liquid nitrogen and stored at -80°C until processing for qRT-PCR of inflammation markers on total RNA extracted using a commercial kit (*e.g.*, RNeasy Lipid Tissue, Qiagen).

1. Add a glass bead to the hemisphere in 1 ml of Trizol in a 1.5 ml Eppendorf tube.
2. Homogenize samples using a TissueLyser device.
3. Add 200 μl s of chloroform to homogenate and mix at 21°C .
4. Centrifuge at $14,000 \times g$ for 15 min at 4°C .
5. Transfer 500 μl of the supernatant to a fresh Eppendorf tube and add 500 μl of 70% ethanol.
6. Process for total RNA extraction, following the [manufacturer's instructions](#). Determine the RNA concentration of the sample eluted in RNase-free water using a Nanodrop device.
7. Perform reverse transcription using the Reverse Transcription kit, and quantitative PCR using the SYBR Green PCR master Kit, following the manufacturer's instructions, with the the QuantiTect Primer assays or the following primers for GFAP: 5'-GGGGCAAAGCACCAAGAAG-3' and 5'-GGGACAACCTTGATTGTGAGCC-3'. Results are typically expressed as a ratio relative to values obtained for 18S RNA control (Figure 2).

E. Brain slice preparation, immuno-fluorescence staining, and analysis with confocal fluorescence microscopy (Figure 3)

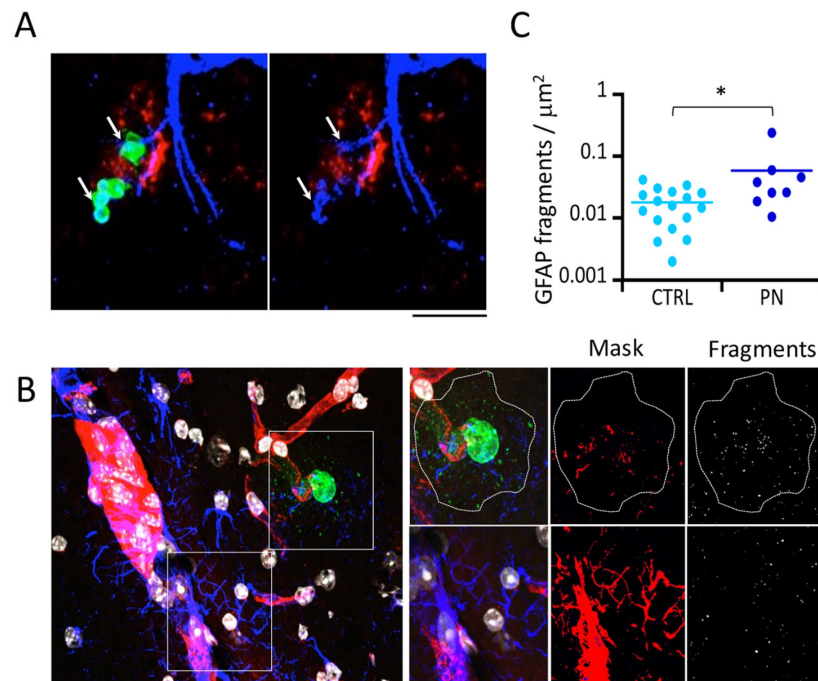


Figure 3. Confocal microscopy analysis of GFAP-labeled brain slices.

C57/BL6 6-8-week-old mice were injected intravenously with 10^7 PN equivalent CFUs via the RO sinus. Brains were excised at 6 h post-infection, and 20 μm thick brain slices were cut with a cryostat for immunofluorescence staining. **A.** Representative maximal projections of confocal planes. Arrows:

PN-associated GFAP fragmentation. Green: PN capsule; blue: GFAP; red: Isolectin IB-4; gray levels: nuclear DNA. **B.** Right: higher magnification of insets shown in the left panel. Dotted outline: area corresponding to PN microcolony and capsular remnants (PN-CS) associated with fragmentation of the GFAP filament network. Right panels: GFAP fragments are detected using the particle analysis plug-in of Fiji (Methods). **C.** Quantification of GFAP fragments per μm^2 in PN-CS (PN) or control area (CTRL) (N = 2, > 10,000 fragments). Mann and Whitney. *: $P < 0.05$. Scale bar = 5 μm .

1. Embed freshly dissected hemispheres in OCT, frozen in isopentane at -25°C , and stored at -80°C or sectioned.
2. Perform sequential 20 μm coronal sections of the frozen hemispheres in a cryostat.
3. Lay slices in an orderly manner onto slides, so as to keep track of the corresponding brain area. These records are subsequently used to analyze whether PN crossing of the BBB occurs at specific sites.
4. Fix brain slices in 4% paraformaldehyde diluted in PBS for 15 min at 21°C . All subsequent steps are performed at 21°C .
5. Permeabilize samples for 60 min in PBS containing 0.25 % Triton X-100 and 5% newborn goat serum (NGS), then wash three times in PBS. The use of a slide holder enabling the simultaneous dipping of samples in successive beakers is convenient for the processing of multiple samples.
6. Perform incubation with the primary antibodies at the following dilutions: anti-GFAP (1:500); anti-PN capsular (1:300); AlexaFLuor 568-IB4 (1:100), in PBS containing 5% NGS, for 60 min in a humid chamber or staining tray. Minimizing incubation volume can be conveniently performed by carefully draining excess PBS after the last wash by capillarity, placing the slide orthogonally with the slide edge contacting a paper towel. The slide is placed face-up, and 20 μl s of the primary antibody solution is placed on each brain slice. A piece of parafilm or 13 mm – diameter coverslip is placed on top of the drop to enable antibody distribution over the slice and limit evaporation.
7. Remove parafilm or coverslip.
8. Wash samples three times in PBS.
9. Perform incubation with the secondary Alexa-conjugated secondary antibodies, Phalloidin used at a 1:200 dilution, and DAPI used at 100 μg /ml final concentration for 60 min in a humid chamber or staining tray.
10. Wash samples three times in PBS.
11. Add 20 μl of DAKO fluorescence mounting medium above each slice and place a 13 mm-diameter coverslip.
12. Allow DAKO to polymerize for at least 30 min in the dark. Samples should be stable to store in the dark for several weeks.
13. Samples are analyzed using Eclipse Ti inverted microscopes equipped with a 60 \times oil immersion objective, a CSU1-W1 spinning disk confocal head, and an ORCA Flash 4.0 CMOS camera

controlled by the Metamorph 7.7 software. The large chip of this camera (2,048 pxl × 2,048 pxl) enables visualization of large regions of brain slices, facilitating the analysis of rare events such as PN translocation across the BBB at early time-points. For example, at 6 h post-infection, we detected a PN translocation in the brain cortex in about 1 field out of one hundred 60× objective fields.

F. Image acquisition

The anti-PN capsular staining provides a clear contrast enabling the unambiguous detection of bacteria in brain slices (Figure 3). However, this unambiguous detection requires the 3D-analysis of the slice, and therefore acquisitions of Z-planes covering the 20 μm width of the brain slice. The procedure can become challenging when several fluorophores are analyzed because of the lengthening of the acquisition procedure and potential bleaching linked to repeated sample illumination; thus, particular basic care should be taken as for all quantitative acquisitions. We will not discuss here automation procedures enabling the 3D-acquisition of adjacent fields that can be advantageously applied when a programmable motorized microscopy stage is available.

1. To limit oversampling of focal planes, and because PN roughly corresponds to 1 μm diameter cocci, an inter-plane spacing of 400 nm secures bacterial detection along the slice width.
2. Acquisition parameters need to be determined empirically for each fluorophore. Because the acquisition parameters cannot be changed during the analysis of a given sample, they should be determined for each fluorophore and fixed prior to the beginning of large-scale acquisition. Ideally, a preliminary sample analysis on the dimmest and brightest object is used to set up the optimal exposure time while preventing saturation.
3. When fluorescence intensity is limiting, favor increasing exposure time over laser power to help limit photobleaching. Acquisitions for fluorophores for which quantification of intensity is sensitive should be performed first.
4. When the laser power and exposure time are set for each fluorophore, proceed with the acquisition of adjacent planes. Usual exposure time for average intensity fluorescent signals ranges between 200 and 400 ms for a C-MOS camera. If 50 focal planes are acquired for four different fluorophores, acquisition of each field may take from 2-4 min.

G. Image analysis

In our analysis, we focus on PN translocation across brain parenchymal blood vessels and its effects on the astrocytic glial fibrillary acid protein (GFAP) intermediate filament network. Specifically, the parameters analyzed are the association of PN clusters with blood vessels and the fragmentation of GFAP associated with translocated PN clusters. For these parameters, while care is taken to preserve fluorescence to detect stained structures, quantification of fluorescence intensity is not performed. These considerations are important when converting the acquired Z-stacks into 2D-image maximal projections. GFAP staining shows a typical filamentous network, corresponding to

astrocytic processes. Fragmentation of GFAP filaments is observed at the levels of processes contacting bacteria (Figure 3A, arrows). For bigger PN clusters, GFAP fragmentation is also observed at the distant vicinity of the bacterial cluster. We therefore quantified PN-induced GFAP fragmentation in the area associated with PN clusters delimited by the staining of capsular shedding (Figure 3B, dotted area).

1. Perform maximal projections of stacks for all fluorophores in ImageJ. In the “Image” menu, select “Stacks,” then “Z project,” then “maximal projection.”
2. Combine corresponding images by adjusting the luminosity/contrast display for each fluorophore. As shown in Figure 3A, PN clusters are clearly detected extruding from brain vessels into the brain matter at 6 h post-infection. An association of 100% with blood vessels labeled with isolectin IB-4 is established for all PN clusters detected at 6 h and 13 h post-infection (Figure 3).
3. The GFAP channel image is converted into a 8-bit image.
4. A binary mask of the image is performed by setting a threshold. In doing so, pay attention that the overlaid structures faithfully match the detected GFAP fragments (Figure 3).
5. Use the PN capsular staining channel to delimit the area corresponding to capsular shedding.
6. Transfer this area to the image corresponding to the GFAP channel.
7. Run the particle analysis Fiji plug-in with the following parameters: particle size > 0.05 μm^2 and a circularity index > 0.9.
8. Normalize the number of detected GFAP fragments to the area.
9. Statistical difference between animal groups is evaluated with a non-parametric test.

Acknowledgments

The work was funded in part by the ANR project CALPLYCX (Grant number: ANR-20-CE15-0001). This protocol was adapted from Bello *et al.* (2020).

Competing interests

The authors declare no competing interests.

Ethics

Experiments and techniques reported here complied with the ethical rules of the French agency for animal experimentation and with the Institute of Drugs, Toxicology, Chemistry, and the Environment animal ethics committee (Paris Descartes University, Agreement 86-23).

References

1. Abbott, N. J. and Friedman, A. (2012). [Overview and introduction: the blood-brain barrier in health and disease](#). *Epilepsia* 53 Suppl 6: 1-6.
2. Abbott, N. J., Patabendige, A. A., Dolman, D. E., Yusof, S. R. and Begley, D. J. (2010). [Structure and function of the blood-brain barrier](#). *Neurobiol Dis* 37(1): 13-25.
3. Armulik, A., Genove, G., Mae, M., Nisancioglu, M. H., Wallgard, E., Niaudet, C., He, L., Norlin, J., Lindblom, P., Strittmatter, K., *et al.* (2010). [Pericytes regulate the blood-brain barrier](#). *Nature* 468(7323): 557-561.
4. Bello, C., Smail, Y., Sainte-Rose, V., Podglajen, I., Gilbert, A., Moreira, V., Chretien, F., Cohen Salmon, M. and Tran Van Nhieu, G. (2020). [Role of astroglial Connexin 43 in pneumolysin cytotoxicity and during pneumococcal meningitis](#). *PLoS Pathog* 16(12): e1009152.
5. Cucullo, L., Hossain, M., Puvenna, V., Marchi, N. and Janigro, D. (2011). [The role of shear stress in Blood-Brain Barrier endothelial physiology](#). *BMC Neurosci* 12: 40.
6. GBD 2016 Meningitis Collaborators, (2018). [Global, regional, and national burden of meningitis, 1990-2016: a systematic analysis for the Global Burden of Disease Study 2016](#). *Lancet Neurol* 17(12): 1061-1082.
7. Gerlini, A., Colomba, L., Furi, L., Braccini, T., Manso, A. S., Pammolli, A., Wang, B., Vivi, A., Tassini, M., van Rooijen, N., *et al.* (2014). [The role of host and microbial factors in the pathogenesis of pneumococcal bacteraemia arising from a single bacterial cell bottleneck](#). *PLoS Pathog* 10(3): e1004026.
8. Grandgirard, D., Steiner, O., Täuber, M. G. and Leib, S. L. (2007). [An infant mouse model of brain damage in pneumococcal meningitis](#). *Acta Neuropathol* 114(6): 609-617.
9. Gres, V., Kolter, J., Erny, D. and Henneke, P. (2019). [The role of CNS macrophages in streptococcal meningoencephalitis](#). *J Leukoc Biol* 106(1): 209-218.
10. Haruwaka, K., Ikegami, A., Tachibana, Y., Ohno, N., Konishi, H., Hashimoto, A., Matsumoto, M., Kato, D., Ono, R., Kiyama, H., *et al.* (2019). [Dual microglia effects on blood brain barrier permeability induced by systemic inflammation](#). *Nat Commun* 10(1): 5816.
11. Iovino, F., Orihuela, C. J., Moorlag, H. E., Molema, G. and Bijlsma, J. J. (2013). [Interactions between blood-borne *Streptococcus pneumoniae* and the blood-brain barrier preceding meningitis](#). *PLoS One* 8(7): e68408.
12. Jeong, D. G., Jeong, E. S., Seo, J. H., Heo, S. H. and Choi, Y. K. (2011). [Difference in Resistance to *Streptococcus pneumoniae* Infection in Mice](#). *Lab Anim Res* 27(2): 91-98.
13. Kulohoma, B. W., Cornick, J. E., Chaguza, C., Yalcin, F., Harris, S. R., Gray, K. J., Kiran, A. M., Molyneux, E., French, N., Parkhill, J., *et al.* (2015). [Comparative Genomic Analysis of Meningitis- and Bacteremia-Causing Pneumococci Identifies a Common Core Genome](#). *Infect Immun* 83(10): 4165-4173.
14. Mook-Kanamori, B. B., Geldhoff, M., van der Poll, T. and van de Beek, D. (2011). [Pathogenesis and pathophysiology of pneumococcal meningitis](#). *Clin Microbiol Rev* 24(3): 557-591.

15. Sandgren, A., Albiger, B., Orihuela, C. J., Tuomanen, E., Normark, S. and Henriques-Normark, B. (2005). [Virulence in mice of pneumococcal clonal types with known invasive disease potential in humans](#). *J Infect Dis* 192(5): 791-800.
16. Shahum, A., Holeckova, K., Lesnakova, A., Streharova, A., Karvaj, M., Steno, J., Rudinsky, B., Bauer, F., Huttova, M., Bielova, M., *et al.* (2007). [Bacteremic meningitis is associated with inferior outcome in comparison to community acquired meningitis without bacteremia](#). *Neuro Endocrinol Lett* 28 Suppl 3: 25-26.
17. Sonar, S. A. and Lal, G. (2018). [Blood-brain barrier and its function during inflammation and autoimmunity](#). *J Leukoc Biol* 103(5): 839-853.
18. Wu, J., Cai, Y., Wu, X., Ying, Y., Tai, Y. and He, M. (2021). [Transcardiac Perfusion of the Mouse for Brain Tissue Dissection and Fixation](#). *Bio-protocol* 11(5): e3988.
19. Yardeni, T., Eckhaus, M., Morris, H. D., Huizing, M. and Hoogstraten-Miller, S. (2011). [Retro-orbital injections in mice](#). *Lab Anim (NY)* 40(5): 155-160.
20. Zuluaga-Ramirez, V., Rom, S. and Persidsky, Y. (2015). [Craniula: A cranial window technique for prolonged imaging of brain surface vasculature with simultaneous adjacent intracerebral injection](#). *Fluids Barriers CNS* 12: 24.